Extraction of Weak Transition Strengths via the (^{3}He, t) Reaction at 420 MeV

R. G. T. Zegers,[1,2,3] T. Adachi,[4] H. Akimune,[5] Sam M. Austin,[1,3] A. M. van den Berg,[6] B. A. Brown,[1,2,3] Y. Fujita,[7] M. Fujiwara,[8,4] S. Galès,[9] C. J. Guess,[1,2,3] M. N. Harakeh,[6] H. Hashimoto,[4] K. Hatanaka,[4] R. Hayami,[10] G. W. Hitt,[1,2,3] M. E. Howard,[3,11] M. Itoh,[12] T. Kawabata,[13] K. Kawase,[8] M. Kinoshita,[5] M. Matsubara,[4] K. Nakanishi,[4] S. Nakayama,[10] S. Okumura,[4] T. Ohta,[4] Y. Sakemi,[4] Y. Shimbara,[1] Y. Shimizu,[4] C. Scholl,[14] C. Simenel,[1,15] Y. Tameshige,[4] A. Tamii,[4] M. Uchida,[16] T. Yamagata,[5] and M. Yosoi[4]

[1]*National Superconducting Cyclotron Laboratory, Michigan State University, East Lansing, Michigan 48824-1321, USA*
[2]*Department of Physics and Astronomy, Michigan State University, East Lansing, Michigan 48824, USA*
[3]*Joint Institute for Nuclear Astrophysics, Michigan State University, East Lansing, Michigan 48824, USA*
[4]*Research Center for Nuclear Physics, Osaka University, Ibaraki, Osaka 567-0047, Japan*
[5]*Department of Physics, Konan University, Kobe, Hyogo, 658-8501, Japan*
[6]*Kernfysisch Versneller Instituut, University of Groningen, Zernikelaan 25, 9747 AA Groningen, The Netherlands*
[7]*Department of Physics, Osaka University, Toyonaka, Osaka 560-0043, Japan*
[8]*Kansai Photon Science Institute, Japan Atomic Energy Agency, Kizu, Kyoto 619-0215, Japan*
[9]*Institut de Physique Nucléaire, IN2P3-CNRS, Orsay, France*
[10]*Department of Physics, University of Tokushima, Tokushima 770-8502, Japan*
[11]*Department of Physics, The Ohio State University, Columbus, Ohio 43210, USA*
[12]*Cyclotron and Radioisotope Center, Tohoku University, Sendai, Miyagi 980-8578, Japan*
[13]*Center for Nuclear Study, University of Tokyo, RIKEN Campus, Wako, Saitama 351-0198, Japan*
[14]*Institut für Kernphysik, Universität zu Köln, D-50937 Cologne, Germany*
[15]*CEA/DSM/DAPNIA/SPhN, F-91191 Gif-sur-Yvette, France*
[16]*Tokyo Institute of Technology, 2-12-1 O-Okayama, Tokyo 152-8550, Japan*

(Received 18 July 2007; published 15 November 2007)

Differential cross sections for transitions of known weak strength were measured with the (^{3}He, t) reaction at 420 MeV on targets of ^{12}C, ^{13}C, ^{18}O, ^{26}Mg, ^{58}Ni, ^{60}Ni, ^{90}Zr, ^{118}Sn, ^{120}Sn, and ^{208}Pb. Using these data, it is shown that the proportionalities between strengths and cross sections for this probe follow simple trends as a function of mass number. These trends can be used to confidently determine Gamow-Teller strength distributions in nuclei for which the proportionality cannot be calibrated via β-decay strengths. Although theoretical calculations in the distorted-wave Born approximation overestimate the data, they allow one to understand the main experimental features and to predict deviations from the simple trends observed in some of the transitions.

DOI: 10.1103/PhysRevLett.99.202501 PACS numbers: 25.55.Kr, 21.60.Cs, 24.50.+g, 25.40.Kv

The (^{3}He, t) charge-exchange (CE) reaction is widely used to study the spin-isospin response of nuclei [1,2]. In particular, Gamow-Teller transitions (GT; transfer of spin $\Delta S = 1$, of orbital angular momentum $\Delta L = 0$ and of total angular momentum $\Delta J = 1$) have been the subject of intensive investigations, since they are used to extract weak transition strengths in excitation-energy regions inaccessible to β-decay. These strength distributions are crucial for understanding such diverse topics as late stellar evolution [3,4], neutrino nucleosynthesis [5], design of neutrino detectors [6] and for constraining calculations of matrix elements for (neutrinoless) double β-decay [7,8].

Compared to the (p, n) reaction, use of the (^{3}He, t) reaction at intermediate energies has the distinct advantage that much better energy resolutions (as low as 20 keV [9]) can be achieved. This permits a cleaner extraction of GT strengths (B(GT)) from competing transitions and provides a higher level of detail. However, unlike for the (p, n) reaction, there has been no convincing systematic evaluation of the reliability of extracting B(GT) values using the (^{3}He, t) reaction. Such an evaluation is crucial for obtaining reliable inputs for the above-mentioned applications and for use of the inverse reaction (t, ^{3}He) to extract electron capture strengths [10,11].

In this Letter, we fill this gap by measuring the differential cross sections for the (^{3}He, t) reaction at $E(^3\mathrm{He}) = 420$ MeV on target nuclei over a wide mass range. The data are used to study the (^{3}He, t) reaction mechanism and procedures for extracting B(GT). We find, and understand, differences from the (p, n) reaction and show that the accuracy of the extracted B(GT) values are comparable for the two probes.

The extraction of weak transition strengths from CE data is based on the close proportionality between the weak transition strength and the CE differential cross section at zero momentum transfer [$\frac{d\sigma}{d\Omega}(q = 0)$] derived in the Eikonal approximation [12]. For GT transitions

$$\frac{d\sigma}{d\Omega}(q = 0) = KN_{\sigma\tau}|J_{\sigma\tau}|^2 B(\mathrm{GT}) = \hat{\sigma}_{\mathrm{GT}} B(\mathrm{GT}). \quad (1)$$

Here, K is a kinematical factor, $N_{\sigma\tau}$ a distortion factor defined by the ratio of distorted-wave to plane-wave cross

sections, and $|J_{\sigma\tau}|$ is the volume-integral of the central $\sigma\tau$ interaction. The factor $KN_{\sigma\tau}|J_{\sigma\tau}|^2$ is referred to as the unit cross section, $\hat{\sigma}_{\mathrm{GT}}$. For Fermi transitions ($\Delta S = 0$, $\Delta L = 0$, $\Delta J = 0$), $|J_{\sigma\tau}|$ has to be replaced by $|J_\tau|$, $B(\mathrm{GT})$ by $B(F)$ and $N_{\sigma\tau}$ by N_τ and the unit cross section is referred to as $\hat{\sigma}_F$. The validity of Eq. (1) was studied for the (p, n) reaction [12] on a wide variety of target nuclei at beam energies above $E_p = 120$ MeV. This study made use of transitions for which the $B(\mathrm{GT})$ values are known from β-decay experiments. For Fermi transitions, the sum-rule strength ($B(F) = N - Z$) is nearly exhausted by the excitation of the isobaric analog state (IAS) [13].

The (^{3}He, t) and (p, n) reactions differ significantly. The ^{3}He (t) has internal structure and is absorbed at the surface of the target nucleus, whereas the proton (neutron) is a single nucleon that probes the nuclear interior. Differences between the two probes have become apparent in experimental studies of the ratio $\frac{\hat{\sigma}_{\mathrm{GT}}}{\hat{\sigma}_F}$. Whereas it is nearly independent of mass number for the (p, n) reaction [12], a significant increase has been observed for the (^{3}He, t) reaction [14] that, until now, was poorly understood. Such issues have led to concerns about the validity of Eq. (1) for the (^{3}He, t) reaction at ~420 MeV. Moreover, extraction of GT strengths when the unit cross section can not be calibrated using known strengths from β-decay, at present has poorly known errors.

To provide the necessary systematics, accurate absolute differential cross sections at forward scattering angles for transitions for which the Fermi or GT strengths are known were obtained in two experiments performed at RCNP. In the first experiment, the (^{3}He, t) reaction on ^{12}C, ^{13}C, ^{18}O, ^{26}Mg, ^{60}Ni, ^{90}Zr, ^{120}Sn, and ^{208}Pb was measured. The tritons were detected in the focal plane of the Grand Raiden spectrometer [15] up to laboratory scattering angles of 2.5°. The experiment was run in achromatic and off-focus [16] modes of operation and resolutions in excitation energy of 100 keV (FWHM) and scattering angle of 0.2° were achieved (for details, see Ref. [17] in which the ^{26}Mg(^{3}He, t) data are discussed in detail). The systematic uncertainty in absolute cross sections was about 10%, mainly due to uncertainties in the beam-current integration using a Faraday cup.

In the second experiment, cross sections on ^{26}Mg, ^{58}Ni, and ^{118}Sn were measured up to 4°. The experiment was performed in dispersion-matched mode [18], resulting in energy resolutions of ~40 keV (FWHM). The ^{26}Mg data were used to check for consistency with the first experiment. Angular distributions measured in the two experiments were found to be in good agreement, but due to inefficient current integration when running in dispersion-matched mode, a 20% correction had to be applied to all cross sections measured in the second experiment.

The differential cross sections were extracted for transitions to final states with known GT and Fermi strengths listed in Table I. For the case of ^{13}C, results from Ref. [21] were also used in the analysis. The extraction of the cross section for the excitation of the IAS in ^{13}N required special care, since the transition to the $\frac{1}{2}^-$ ground state contains both GT and Fermi contributions. The GT contribution was removed using the GT unit cross section extracted from the excitation of the $\frac{3}{2}^-$ state at 15.1 MeV, for which the $B(\mathrm{GT})$ is determined from the β^--decay of its isospin multiplet partner ^{13}B [12].

As an example of the procedure for extracting unit cross sections, the results for the Fermi and GT transitions from ^{58}Ni to ^{58}Cu are shown in Fig. 1. Figure 1(a) shows the part of the excitation-energy spectrum that includes the GT transition of known strength to the 1^+ ground state and the Fermi transition to the 0^+ state at 0.203 MeV. Their differential cross sections are plotted in Figs. 1(b) and 1(c), respectively. To extract the cross section at 0°, the experimental differential cross sections are fitted to theoretical ones, calculated in the distorted-wave Born approximation (DWBA) using the code FOLD [22].

For the optical potentials, parameters that are extracted from ^{3}He elastic scattering data [23,24] were used (the data from Ref. [23] were refitted). The effective nucleon-nucleon interaction of Love and Franey [25] is double folded over the transition densities of the ^{3}He-^{3}H and target-residual systems. For ^{3}He and ^{3}H, densities were obtained from variational Monte Carlo results [26]. For the target-residual system, one-body transition densities (OBTDs) were calculated with the shell-model code OXBASH [27] and obtained from Ref. [28], using appropriate interactions for the nuclei in Table I. For Fermi transitions in nuclei heavier than ^{26}Mg, OBTDs were determined from a normal-modes procedure [29]. Details on the DWBA calculations can be found in Refs. [11,17] and will be discussed in a forthcoming publication.

In the case of Fermi transitions [Fig. 1(c)] a single fit parameter was used to scale the theory to the data. The extracted 0° cross section was then extrapolated to $q = 0$ using the ratio of calculated cross sections in DWBA at

TABLE I. Transitions to final states included in the analysis of the GT and Fermi unit cross sections. The $B(\mathrm{GT})$ values were calculated from known log ft values [19] following Ref. [20]. For the Fermi strengths, $B(F) = N - Z$ was used.

GT		Fermi	
(J^π, E_x [MeV])	$B(\mathrm{GT})$	(J^π, E_x [MeV])	$B(F)$
^{12}N(1^+, 0.)	0.88	^{13}N($\frac{1}{2}^-$, 0.)	1
^{13}N($\frac{3}{2}^-$, 15.1)	0.23	^{26}Al(0^+, 0.228)	2
^{18}F(1^+, 0.)	3.11	^{58}Cu(0^+, 0.203)	2
^{26}Al(1^+, 1.06)	1.10	^{60}Cu(0^+, 2.54)	4
^{58}Cu(1^+, 0.)	0.155	^{90}Zr(0^+, 5.01)	10
^{118}Sb(1^+, 0.)	0.344	^{118}Sb(0^+, 9.3)	18
^{120}Sb(1^+, 0.)	0.345	^{120}Sb(0^+, 10.2)	20
		^{208}Bi(0^+, 15.1)	44

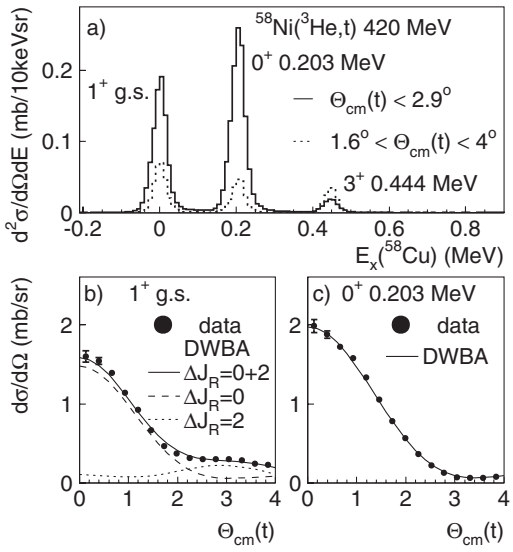

FIG. 1. (a) Low-energy part of the excitation-energy spectrum in ^{58}Cu measured via ^{58}Ni(^{3}He, t) at 420 MeV. The full line (dashed line) corresponds to the spectrum taken with the spectrometer set at 0° (2.5°). (b) Measured differential cross section for the GT transition to the 1^+ ground state and fit with DWBA angular distribution. (c) Idem for the Fermi transition to the 0^+ state at 0.203 MeV. Error bars are statistical only and mostly smaller than the dots.

$q = 0$ and 0°. Of the transitions (Fermi and GT) studied here, this ratio was maximally 1.25. For the GT transitions, a similar procedure was used. However, the analysis is complicated by contributions from incoherent and coherent $\Delta L = 2$, $\Delta S = 1$ contributions to the $\Delta J = 1$ GT excitation. The incoherent contribution, due to a transition in which the total angular momentum transfer (ΔJ_R) to the relative motion between the target and projectile equals 2, was removed by fitting the angular distribution to a linear combination of the theoretical $\Delta J_R = 0$ and $\Delta J_R = 2$ components calculated in DWBA, as shown in Fig. 1(b). Only the $\Delta J_R = 0$ component is used to determine the 0° GT cross section. The coherent contribution, largely due to the noncentral tensor-interaction and the largest source that breaks the proportionality of Eq. (1) [9,11,17], cannot easily be determined from the data since it does not strongly affect the angular distribution at forward scattering angles. We estimated its effect on the cross sections using the ratio of the DWBA calculations with and without the tensor force. Such estimates have proven to provide reasonable predictions for the proportionality breaking in ^{26}Mg [17] and ^{58}Ni [11]. For two of the cases studied here, effects larger than statistical errors were predicted. For the excitation of the ^{58}Cu(1^+) state, the cross section decreased by 20% if the tensor force was excluded from the calculation. To correct for this, the GT unit cross section extracted from the data should be reduced by 20% [11]. For the GT component of the excitation of the ^{13}N ground state (needed for extraction of the Fermi strength in this transition, see above), the cross section decreased by 15% if the tensor force was excluded. Its cross section estimate, based on the unit cross section extracted from the 15.1 MeV state in ^{13}N, must thus be increased by that percentage before subtracting it from the total ground-state cross section for the purpose of deducing the cross section of the Fermi component. Consequently, the Fermi unit cross section decreases. We initially ignore these corrections and then show how they affect the relevant unit cross sections.

The unit cross sections $\hat{\sigma}_{\mathrm{GT}}$ and $\hat{\sigma}_F$ are calculated by dividing the extracted cross sections at $q = 0$ by the known $B(\mathrm{GT})$ and $B(F)$ values, respectively. In Fig. 2(a) the empirical Fermi unit cross sections are plotted against mass number. A very smooth decreasing trend is seen which is well fitted with the function $\hat{\sigma}_{F,\mathrm{fit}} = 72/A^{1.06}$. By dividing the measured Fermi unit cross sections by $\hat{\sigma}_{F,\mathrm{fit}}$ [Fig. 2(b)] it is seen that the experimental unit cross sections deviate by no more than 15% from the fit, except for the case of the IAS in ^{13}N. After the above-mentioned correction to GT component of this transition, the Fermi unit cross section for this nucleus decreases by an amount indicated by the arrow in Fig. 2(b) and its corrected value is close to the trend line.

In both Figs. 2(a) and 2(b), the theoretical unit cross section calculated by dividing the DWBA cross sections at $q = 0$ for each transition by $B(F) = N - Z$ are also shown. The trend follows the data, but the values are

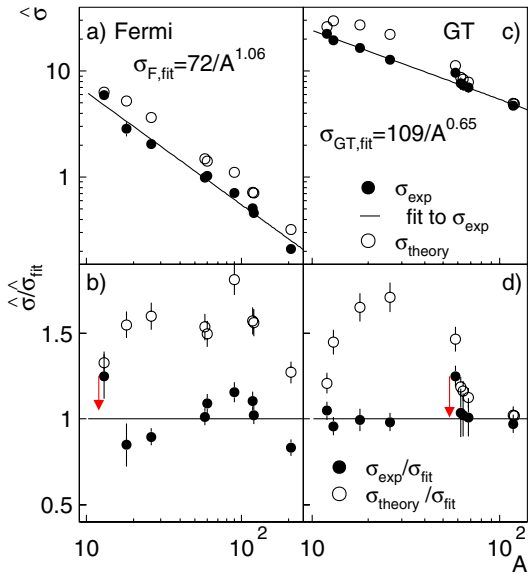

FIG. 2 (color online). (a) Mass dependence of the experimental and theoretical Fermi unit cross sections. The line indicates a fit to the experimental values. (b) Relative deviation of the experimental and theoretical Fermi unit cross sections from the fitted mass dependence in (a). (c) As in (a), but for the GT unit cross sections. (d) As in (b), but for the GT unit cross sections. The arrows in (b) (for ^{13}C) and (d) (for ^{58}N) indicate to which value these unit cross section change after theoretically estimated corrections are applied (see text).

30%–80% too high. Further development of the reaction codes is needed to understand this discrepancy, but likely sources are the approximate treatment of exchange [30], density dependence of the nucleon-nucleon interaction and uncertainties in the optical potentials.

In Figs. 2(c) and 2(d), similar plots are shown for the GT unit cross sections. To complement the results, GT unit cross sections for $A = 62$, 64 and 68 were calculated by multiplying measured $\frac{\hat{\sigma}_{\mathrm{GT}}}{\hat{\sigma}_F}$ ratios [4] by the $\hat{\sigma}_{F,\mathrm{fit}}$ fit function described above. The mass number dependence of the GT unit cross section is well fitted with the function $\hat{\sigma}_{\mathrm{GT},fit} = 109/A^{0.65}$ [Fig. 2(c)] and the measured GT unit cross sections deviate by no more than 5% from this function, except for ^{58}Cu. After the above-mentioned correction, the unit cross section for this case reduces (see arrow in Fig. 2(d)] to a value close to the trend line. The theoretical GT unit cross sections, calculated by dividing the $\Delta L = 0$ DWBA cross sections at $q = 0$ for each transition by its corresponding theoretical B(GT) overestimate the data by up to 70%, with the largest deviations seen for medium-mass nuclei.

It is important to note that the τ component of the nucleon-nucleon interaction is short-range in nature, whereas the $\sigma\tau$ component is dominated by long-range terms [25]. The difference in range between the two is responsible for the different dependences of GT and Fermi unit cross sections (and thus their ratio [14]) on mass number and this is seen in both theory and data. The long-range nature of the $\sigma\tau$ interaction partially counters the strong absorption of the probe on the surface of the nucleus and this effect becomes stronger for heavier nuclei. The (p, n) reaction is different in this regard since it probes the interior of the nucleus. Consequently, the difference in range between τ and $\sigma\tau$ components matters less and the empirical target mass dependences of Fermi and GT unit cross sections are very similar [12].

In summary, we have analyzed absolute differential cross sections over a wide mass range and found that the empirical mass dependences of Fermi and GT unit cross sections for the (^{3}He, t) reaction at 420 MeV are well described by simple relationships. This puts the use of this probe to extract weak transition strengths on a solid phenomenological footing and makes it possible to extract with confidence GT strengths in nuclei for which the unit cross section cannot be calibrated using transitions with known B(GT) from β-decay. The theoretical unit cross sections calculated in distorted-wave Born approximation overestimate the data but are adequate to estimate corrections to GT cross sections due to the noncentral tensor component of the interaction and qualitatively explain the difference in mass dependence between Fermi and GT unit cross sections.

We wish to express our gratitude to the cyclotron staff at RCNP. This work was supported by the US NSF (Nos. PHY-0216783 (JINA), PHY-0606007 and PHY-0555366), the Ministry of Education, Science, Sports and Culture of Japan, the Stichting voor Fundamenteel Onderzoek der Materie (FOM), the Netherlands and the DFG, under contract No. Br 799/12-1.

[1] M. Fujiwara *et al.*, Nucl. Phys. **A599**, 223c (1996).
[2] M. N. Harakeh and A. van der Woude, *Giant Resonances: Fundamental High-Frequency Modes of Nuclear Excitations* (Oxford University, New York, 2001).
[3] Y. Fujita *et al.*, Phys. Rev. Lett. **95**, 212501 (2005).
[4] T. Adachi *et al.*, Phys. Rev. C **73**, 024311 (2006).
[5] A. Byelikov *et al.*, Phys. Rev. Lett. **98**, 082501 (2007).
[6] M. Fujiwara *et al.*, Phys. Rev. Lett. **85**, 4442 (2000).
[7] H. Akimune *et al.*, Phys. Lett. B **394**, 23 (1997).
[8] H. Ejiri, J. Phys. Soc. Jpn. **74**, 2101 (2005).
[9] Y. Fujita *et al.*, Phys. Rev. C **75**, 057305 (2007).
[10] G. W. Hitt *et al.*, Nucl. Instrum. Methods Phys. Res., Sect. A **566**, 264 (2006).
[11] A. L. Cole *et al.*, Phys. Rev. C **74**, 034333 (2006).
[12] T. D. Taddeucci *et al.*, Nucl. Phys. **A469**, 125 (1987).
[13] K. I. Ikeda, S. Fujii, and J. I. Fujita, Phys. Lett. **3**, 271 (1963).
[14] T. Adachi *et al.*, Nucl. Phys. **A788**, 70c (2007).
[15] M. Fujiwara *et al.*, Nucl. Instrum. Methods Phys. Res., Sect. A **422**, 484 (1999).
[16] H. Fujita *et al.*, Nucl. Instrum. Methods Phys. Res., Sect. A **469**, 55 (2001).
[17] R. G. T. Zegers *et al.*, Phys. Rev. C **74**, 024309 (2006).
[18] H. Fujita *et al.*, Nucl. Instrum. Methods Phys. Res., Sect. A **484**, 17 (2002).
[19] Evaluated Nuclear Structure Data File by the National Nuclear Data Center, Brookhaven National Laboratory, on behalf of the international Nuclear Structure Decay Data Evaluators Network; http://www.nndc.bnl.gov).
[20] W.-T. Chou, E. K. Warburton, and B. A. Brown, Phys. Rev. C **47**, 163 (1993).
[21] H. Fujimura *et al.*, Phys. Rev. C **69**, 064327 (2004).
[22] J. Cook and J. Carr (1988), computer program fold, Florida State University (unpublished); based on F. Petrovich and D. Stanley, Nucl. Phys. A **275**, 487 (1977); modified as described in J. Cook *et al.*, Phys. Rev. C **30**, 1538 (1984); R. G. T. Zegers, S. Fracasso, and G. Colò (unpublished).
[23] T. Yamagata *et al.*, Nucl. Phys. **A589**, 425 (1995); T. Yamagata and H. Akimune (private communication).
[24] J. Kamiya *et al.*, Phys. Rev. C **67**, 064612 (2003).
[25] W. G. Love and M. A. Franey, Phys. Rev. C **24**, 1073 (1981); M. A. Franey and W. G. Love, Phys. Rev. C **31**, 488 (1985).
[26] S. C. Pieper and R. B. Wiringa, Annu. Rev. Nucl. Part. Sci. **51**, 53 (2001); R. B. Wiringa (private communication).
[27] B. A. Brown *et al.*, NSCL report No. MSUCL-1289.
[28] M. Honma *et al.*, J. Phys.: Conf. Ser. **20**, 7 (2005); M. Honma (private communication).
[29] M. A. Hofstee *et al.*, Nucl. Phys. A **588**, 729 (1995).
[30] T. Udagawa, A. Schulte, and F. Osterfeld, Nucl. Phys. **A474**, 131 (1987).